European Journal of Soil Science, March 2002, **53,** 83–94

Effect of rain on the macroporosity at the soil surface

S. Rousseva[a], D. Torri[b] & M. Pagliai[c]
[a]*N. Poushkarov Institute for Soil Science, Chaussee Bankya 7, 1080 Sofia, Bulgaria,* [b]*Istituto per la Genesi e l'Ecologia del Suolo, CNR, Piazzale delle Cascine 15, 50144 Firenze, and* [c]*Istituto Sperimentale per lo Studio e la Difesa del Suolo, MiPA, Piazza M. d'Azeglio 30, 50121 Firenze, Italy*

Summary

Rain falling on soil causes slaking, mechanical disruption of aggregates and compaction. Too few data exist to predict the changes likely to occur in particular soil, landscape and management conditions. Experiments with simulated rain were set up to study and to model mathematically the changes of the pore system within the surface layer of a soil when rain was applied on a field cropped with maize. Macroporosity, pore-size and pore-shape distributions, and the pore volume were measured by image analysis of thin sections and the fractal dimensions of the pore surface roughness were estimated. The general trends of changes in porosity indicated the presence of two different sets of processes at the surface (0–3 cm) and in the layer immediately underneath (3–6 cm). In both layers most of the variation in macroporosity was due to a loss of elongated porosity. A theoretical approach recently developed to link rain and erosion to sealing properties was extended to describing the effect of rain on the elongated porosity and the pore volume fractal dimension in these two layers. The resulting set of equations describe in detail the evolution of soil porosity near the soil surface. Our approach could be useful when modelling the effects of sealing processes in soil erosion.

Introduction

When raindrops hit the soil surface they cause mechanical disruption of near-surface aggregates, slaking, dispersion, compaction by their impact, infilling of underlying pores by fine particles and surface sealing. All this is commonly followed by transport and deposition of detached particles and microaggregates. Most studies of these processes have been done during research on sealing and crusting. Many experiments have been conducted to relate specific soil variables such as texture, moisture, aggregate stability, mineralogical composition and surface roughness to the consequences of rain on strength, infiltration, porosity or micromorphology of seal and crust.

Most previous studies aimed to explain what was observed in qualitative terms. Only a few investigators have attempted to measure the properties of seals formed during rain and to link them to the causes using quantitative relations. Tackett & Pearson (1965) showed a gradual increase in bulk density related exponentially to the cumulative rain. Farres (1978) found that the increase of seal thickness during rain was related to the logarithm of the cumulative rain. Boiffin (1984) observed a hyperbolic decrease of the porosity of the upper soil layer with time of exposure to rain. Mualem *et al.* (1990) related the bulk density of soil crusts to the depth from the soil surface by an exponential decay function including a factor describing the particular interaction between rain and soil. They ascribed the maximum change in the bulk density at the surface to the rain's kinetic energy. Roth (1997) showed that the exponential decay function proposed by Mualem *et al.* (1990) better represents the initial stages of surface compaction, whereas the changes in bulk density in the later stages of the formation of structural seals are better described by a sigmoidal function. Bielders & Baveye (1995) linked clay eluviation and the thickness of the 'washed-in' layer to the kinetic energy of rain by linear regressions. In a recent study on the effects of raindrop impact on soil micromorphology under various crop systems, Panini *et al.* (1997) found that most of the reduction in porosity is due to the loss of elongated pores. They developed a simple theoretical approach to link the processes of size reduction of elongated porosity to causative factors through an exponential decay function in a quantitative, physically based manner. The main factors they considered were impacts of drops, infilling of pores, deposition and aggregate thinning. Under the assumptions that (i) transport and deposition of fine grains is proportional to the rate of detachment, and (ii) detachment is proportional to the kinetic energy of impacting drops, Panini *et al.* (1997) derived the following equations for the elongated porosity of

Correspondence: D. Torri. E-mail: dbtorri@iges.fi.cnr.it
Received 16 April 1998; revised version accepted 7 June 2001

a soil layer with constant thickness (seal is defined 'structural' or 'depositional' according to what process is dominating: drop impact and soil detachment or sedimentation, respectively, according to Panini *et al.*, 1997; Bresson & Boiffin, 1990; West *et al.*, 1992):

- for a depositional seal:

$$\Delta P_E = bD, \tag{1}$$

- for a structural seal (drop impact):

$$\Delta P_E = P_{E0}\{1 - \exp(-\kappa_E E)\}, \tag{2}$$

- and for a general seal:

$$\Delta P_E = \alpha bD + (1 - \alpha)P_{ES0}\{1 - \exp(-\kappa D)\}, \tag{3}$$

where Δ represents reduction, P_E is elongated porosity (area per cent), P_{E0} and P_{ES0} (both area per cent) are the initial values of elongated porosity and of elongated porosity where structural seals develop, E is the cumulative energy released by drop impacts per unit of surface [MT^{-2}], D is the cumulative soil detachment [ML^{-2}], α is the fraction of the soil surface that is affected by depositional seal, and b and κ (both being dimensionally [$M^{-1}L^2$]) and κ_E [$M^{-1}T^2$] are coefficients determined by best fitting techniques.

Equation (3) is the weighted mean of the previous two equations under the assumption that the amount of splashed material (detached and deposited) is directly proportional to the kinetic energy of the raindrops. The distinction between initial elongated porosity and the initial elongated porosity below the structural seal arises because the former includes the porosity of the seal layer, whereas the latter does not (see the original paper for a more exhaustive discussion).

Equations (1) and (2) are combined into Equation (4) under the assumption that kinetic energy can be substituted by detachment on the basis that D is directly proportional to E for splash detachment (Ellison, 1947; Poesen & Savat, 1981; Torri *et al.*, 1987; Torri *et al.*, 1998):

$$D = k_S E, \tag{4}$$

where k_S is splash detachability (mass per unit of impacting energy).

If we substitute Equation (4) into Equation (1) we obtain

$$\Delta P = bk_S E. \tag{5}$$

This can be rearranged with Equation (2) into an equivalent of Equation (3):

$$\Delta P = \alpha bk_S E + (1 - \alpha)P_{ES0}\{1 - \exp(-k_E E)\}. \tag{6}$$

This last equation will become useful later in the paper.

The equations proposed by Panini *et al.* (1997) are to be considered a first approach towards a detailed algorithmic description of the evolution of pore systems. Such a description is needed for a better understanding of the processes characterizing interrill areas where sealing is an essential component of soil erosion processes. Sealing depends on some basic process of soil erosion (drop impact, aggregate and particle detachment, transport, deposition, etc.). The changes in the packing of the soil particles and aggregates at the surface changes the detachability of the soil particles and the surface roughness, usually reducing the soil's hydraulic resistance to overland flow. The reduced porosity increases runoff and consequently affects erosion. Hence, as splash erosion, sealing and runoff generation are interacting processes, any complete understanding of soil erosion must necessarily include sealing processes and vice versa.

The modelling approach described by Panini *et al.* (1997) is a starting point on which further work can be built. From now on the set of equations and assumptions on which this approach is based will be called the EP model. As with every model, it can be confuted on the basis of its assumptions and predictions. For example, the variation of porosity due to depositional seal is supposed to consist of the accretion of a depositional layer, characterized by a porosity, over another layer of constant porosity. This is obviously a simplifying assumption, the validity of which can be empirically controlled.

The present stage of development of the EP model does not include anything about the dimension of the pores: it simply states that elongated porosity will be reduced by a certain amount, given a certain impacting energy. As the dimension of pores is also important for defining soil properties such as hydraulic conductivity, the model must include information on the dynamics of some other characteristics of porosity such as pore-size distributions. Consequently, this paper aims at improving the equations of the EP model, evaluating whether the dynamic of porosity varies with depth, and describing the dynamics of the pore-size distribution.

Materials and methods

Rain experiments

We set up an experiment at Fagna Agricultural Experimental Centre (Scarperia, Firenze, Italy) where Panini *et al.* (1997) carried out their experiments. The soil is a Eutric Cambisol (FAO–UNESCO, 1990), indicated as 'Chiesa' in their paper. The particle-size distribution of the A_p horizon is 23% clay, 42.7% silt and 34.3% sand. The bulk density of the upper A_{p1} horizon is 1.4 g cm^{-3}. The experiment was in a maize field, and in this it differed from that of Panini *et al.* (1997), who experimented on bare soil, lucerne and potatoes. The plot was 10 m long and 3.5 m wide, with a gradient of 12%, and was hydraulically isolated by means of metal sheets inserted into the soil to 15 cm depth. Lateral losses due to splash were balanced by soil material splashed inwards as the plot was in the centre of a 14 m-long and 5 m-wide plot irrigated with simulated rain in the same manner.

The rainfall simulator, described by Panini *et al.* (1997), was equipped with 18 axial-flow full cone nozzles (Lechler, Catalogue No 460.888) 6 m above the ground. The simulated rain has a drop distribution similar to that of natural rain, giving good uniformity coefficients for intensity and kinetic energy (Panini *et al.*, 1993). The water fed to the simulator was distilled (electrical conductivity EC $=3\,\mu$S cm^{-1}); it differed from that of Panini *et al.* (1997) who used tap water (EC $\approx 480\,\mu$S cm^{-1}). The intensity was kept constant during the experiments with a mean value of 101 mm hour^{-1} and a kinetic energy rate of 1756 J m^{-2} hour^{-1}. This intensity was selected to accelerate the processes and to use a rain intensity different from the ones used by Panini *et al.* (1997). The simulated rain was applied in two runs: the first lasted 42 minutes (instead of the planned 60 because of a malfunctioning of one pump) and was followed, 24 hours later, by a second one lasting 60 minutes.

Stem flow was determined on eight maize plants. The roughness of the soil (defined according to Onstad, 1984) was measured by means of a profile-meter with sticks spaced at 1.5-cm intervals on six transects (each 90 cm long) before and after the rain. Cohesion was determined by a pocket torvane (shear vane) as the average over sites of structural and depositional features. Slope for splash was estimated from the relative elevation transects using the procedure proposed by Torri *et al.* (1998) and used by Panini *et al.* (1997). The size distribution of soil aggregates stable to water disruption was determined by wet sieving of the sediment sampled during the rain. The grain diameters D_{G50} and D_{G95}, corresponding to the 50th and 95th percentiles of the cumulative size distribution (with $D_{G50} < D_{G95}$), were then calculated.

The area where the plot was established was cultivated with maize (approximately 1.58 m tall) in furrows oriented in the direction of maximum slope. Fifteen days before the experiments the area was harrowed to 10 cm depth. Only a few millimetres of rain fell (less than 10), and no irrigation disturbed the soil surface. The water content (by volume, mean over six replicates) before the first experiment was 9% in the upper 5 cm and 16% at 10 cm depth. Before the second experiment the volumetric water content was 35% at both depths.

The total runoff in 102 minutes of rain (intensity 101 mm hour^{-1}, total precipitation 172 mm) was 24.1 mm, and the total erosion was 0.5 kg m^{-2}, with a sediment load ranging up to 34 g l^{-1} (the average sediment load was 21 g l^{-1}). These values are only indicative because of the presence of open cracks (some of which closed during the experiments) which intercepted part of the overland flow. The mean interrill length was 0.44 m. Mean soil random roughness was 1.30 cm. The slope gradient (tangent) for splash was calculated to be 0.48 m m^{-1} (Torri *et al.*, 1998). Cohesion was 3.34 kPa (measured using a pocket torvane).

Contributions of the throughfall and the water dropping from the canopy were used to determine the kinetic energy of impacting drops, E. The intercepted rain was subdivided into stem flow and drip from leaves. The kinetic energy of impacting drops was calculated as the sum of the kinetic energy of the portion of raindrops that passed untouched through the canopy and that dripping from the leaves, as follows:

$$E(t) = (1 - c_c)E_r(t) + 0.5\rho V_c^2 \int_0^t \{c_c I(t') - F_c(t')d_c\}dt', \quad (7)$$

where c_c is the crop cover (0.56 in our case), E_r is the energy of the rain (J m^{-2}), ρ is water density (kg m^{-3}), V_c is the fall velocity of drops dripping from the crop leaves (m s^{-1}), I is the rain intensity (m hour^{-1}), F_c is the stem flow intensity (m^3 hour^{-1}), d_c is the plant density (4.6 plants m^{-2}), and t is the time from the beginning of the rain (hours). The size of the drops from leaves was estimated after Brandt (1989) as 4 mm. Fall velocity was judged to be 3.6 m s^{-1} (Laws, 1941), considering a mean height of fall of 0.8 m (mean height of dripping leaves). Interception rate (calculated as rain intensity times crop cover) accounted for 56.6 mm hour^{-1}. As stem flow accounted for 44 mm hour^{-1} (2.63 cm^3 s^{-1} per maize plant, mean value over eight observations), the intensity of secondary rain was 12.6 mm hour^{-1}. Thus, the rate of the total impacting energy was determined as 855 J m^{-2} hour^{-1}, while the kinetic energy rate of throughfall was 773 J m^{-2} hour^{-1} and that of canopy drip was 82 J m^{-2} hour^{-1}.

Detachment per unit of impacting energy (detachability, D) was calculated after Torri *et al.* (1998) as

$$D = 0.13(\delta_G D_{G50})/(1.5T)\exp\{-00.36h\ln(6D_{G95}/D_{G50})\} + 1.31\tan\beta + 6.7C, \quad (8)$$

where δ_G is the dry bulk density of the removed particles and aggregates (1500 kg m^{-3}), D_{G50} and D_{G95} (mm) are the grain diameters, corresponding to the 50th and 95th percentiles of the cumulative size distribution of stable grains, T (Pa) is soil cohesion, h (mm) is the depth of water over the soil surface, $\tan\beta$ is the mean slope gradient for splash, and C is clay content (fraction). Detachability was calculated to be 3.2 g J^{-1}. This value is valid if the dispersion of soil particles is negligible because Equation (8) was derived from data collected using simulated rainfall produced with tap water which is usually rich in electrolytes and usually does not disperse the soil. Data collected by Borselli *et al.* (2001) on the effect of water quality on erosion show that when good quality water is used (electrical conductivity of rain water close to 1–2 mS m^{-1}) detachment values of non-saline, non-sodic soils are about 2.3 times the values observed on the same soils using tap water. Hence the detachment value of 3.2 g J^{-1} was increased to 7.4 g J^{-1} to accord with these recent findings.

Macroporosity determinations

Three cores of soil (5 cm diameter, 10 cm high) were taken from the upper 0–10 cm layer before the rain and at four consecutive time intervals during the rain. Sites not affected by surface flow were sampled at the ponding time and at the end of the first rain, then again at the ponding time of the

second rain, and at its end. After drying by acetone replacement (Miedema *et al*., 1974; Murphy, 1986) and impregnation with polyester resin (Crystic SR 17449, Scott Bader Co. Ltd, Wellingborough, UK), vertically oriented thin sections 5 cm × 7 cm were cut from each sample. Three thin sections where selected at each sampling time among those showing no evidence of disturbances due to the whole handling procedure.

The thin sections were analysed using PC Image software (Foster Findlay Associates Ltd, London) to measure total porosity and to characterize pores according to their shape and size. The lateral external edges (width of about 3 mm) of each slide were excluded from the analysis to avoid disturbances due to sampling. The total area of each analysed field, and the areas (A_p) and perimeters (P_p) of detected pores (voids) were measured when the pixel side was calibrated as 29.15 μm. This pixel size implies that the smallest detectable pores were *c*. 60 μm in diameter.

Pores were divided into three shape classes according to their circularity ($P_p^2/4\pi A_p$): regular pores (circularity 1–2), irregular pores (circularity 2–5) and elongated pores (circularity > 5) (Pagliai *et al*., 1983, 1984). These classes correspond approximately to those introduced by Bouma *et al*. (1977). Pores of each shape class were further subdivided into six size classes according to the equivalent pore diameter for regular and irregular pores and the pore width for elongated pores (Pagliai *et al*., 1983, 1984).

We used the algorithms used by Droogers *et al*. (1998) to determine the fractal dimensions. The fractal dimension of the pore volume (D_V) was determined by the box-counting technique applied to the images of thin sections using a reductive algorithm of Mandelbrot (1982):

$$N_{>d} \propto d^{(1-D_V)}, \tag{9}$$

where $N_{>d}$ is the smallest number of pixels with size d that cover the area occupied by pores.

Equation (9) is written in order to incorporate extrapolation from two to three dimensions of the respective fractal dimensions.

The thin sections were also examined by a Zeiss 'R POL' microscope at ×25 magnification to examine the micromorphological structure of the samples.

Results and discussion

Soil structure

Changes in the soil structure are essentially changes in the pore system during the simulated rain. The microscopic examination of thin sections prepared from samples collected just before the rain reveals the presence of crumbly to subangular blocky structure (Figure 1a). This structure changed during the first minutes of rain: the slaking of aggregates caused an interruption of porosity in the top 1 cm of the surface layer,

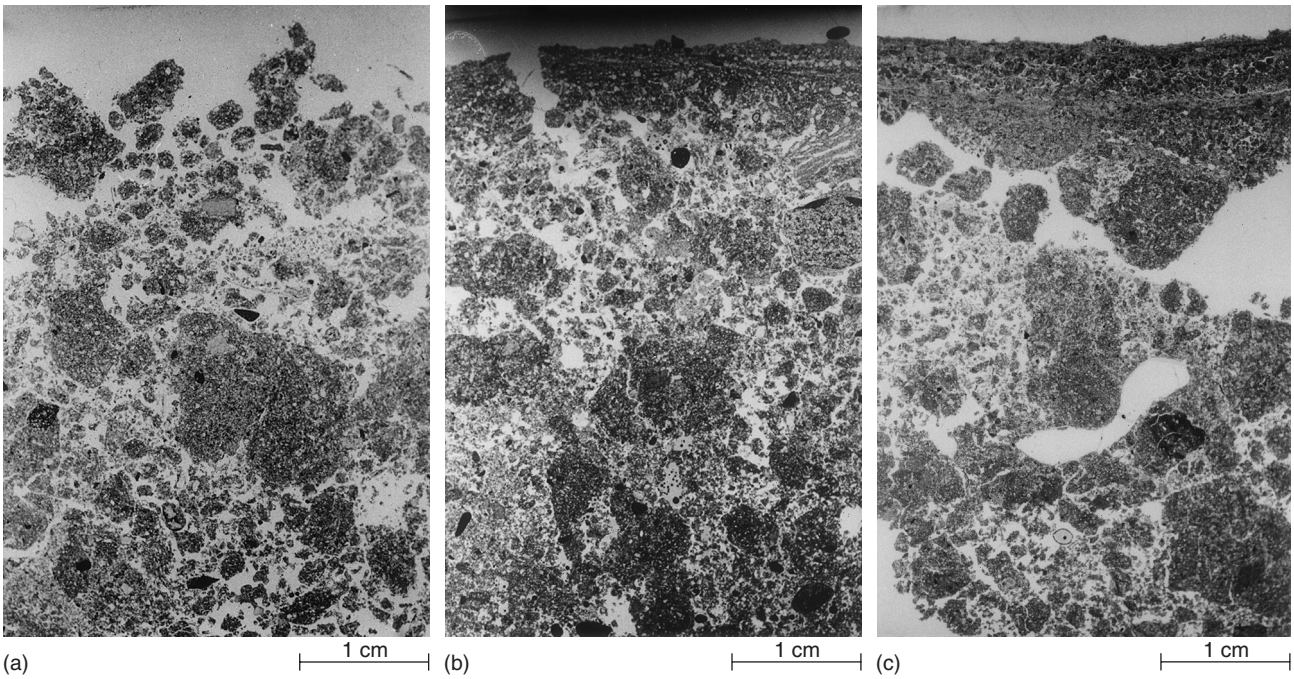

Figure 1 Vertically oriented thin section from samples of the 0–6 cm soil layer: (a) before the rain simulation – a crumbly to subangular blocky structure is evident; (b) after 22 mm rain – the presence of a surface seal is visible; (c) after 71 mm rain. Pictures were taken at ×2 magnification under plain polarized light (parallel Nicols, pores appear white).

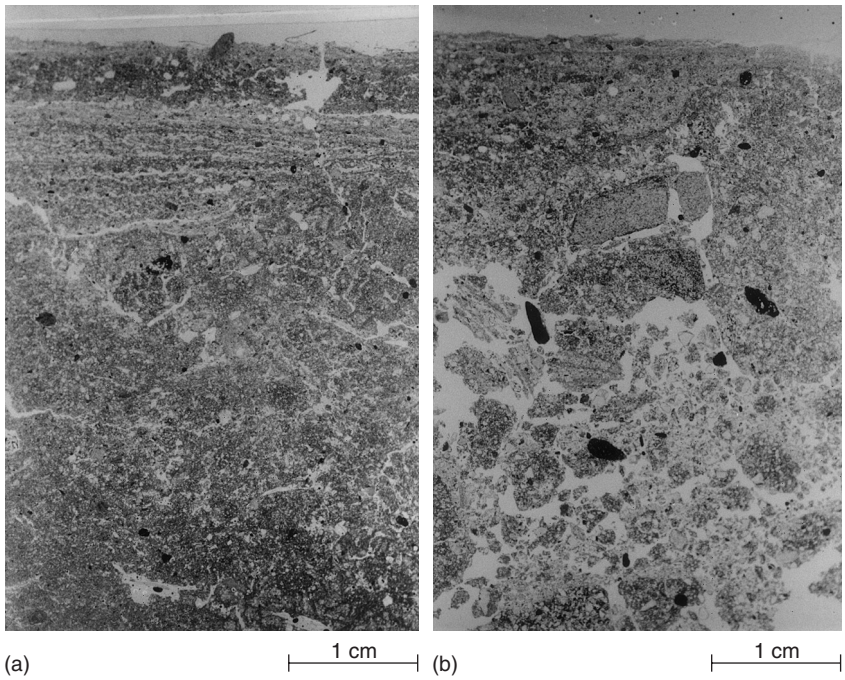

Figure 2 Vertically oriented thin section from samples of the 0–6 cm soil layer after 172 mm rain: (a) depositional seal; (b) structural seal. Pictures were taken at ×2 magnification under plain polarized light (parallel Nicols).

while just below it a subangular blocky structure persists (Figure 1b). At the end of the first simulation a compact surface layer is already evident (Figure 1c) and the subangular blocky structure immediately below has become more compact. During the second simulation the raindrop impact increased the thickness of the compacted surface layer. By the end of the second simulation it had become dense and separated from the subsurface layer by elongated pores oriented parallel to the soil surface both in the depositional (Figure 2a) and in the structural (Figure 2b) seals. Detailed microscopic examination shows that the structural seals have a very compact platy microstructure: thin elongated pores parallel to the soil surface are predominant. Such a microstructure is homogeneously distributed throughout the sealed layer. The microstructure of the depositional seals is characterized by a thin layer of coarse material at the top and a layer of fine material with small, rather porous aggregates below it. Porosity decreases below this latest layer. Generally, porosity is greater in the depositional seal where the proportion of regular and irregular pores is larger than in the structural seal. Such pores are formed mainly by entrapped air, and many of them are spherical.

Macroporosity

To see whether the effect of impacting drops reached much below the soil surface, thin sections were subdivided in an upper (0–3 cm) and an underneath (3–6 cm) layer, called, respectively, S- and U-layer. This subdivision was not based on morphological considerations, but on the fact that both parts would have been sufficiently big to allow enough pores to be examined in both subsamples.

Figure 3 shows the data for regular, irregular and elongated pores in the soil cores sampled at consecutive time intervals during the simulated rain. It appears that (i) the volume of regular and irregular pores in the S-layer does not vary significantly during the rain, (ii) the volume of regular and irregular pores in the U-layer decreases slightly, but trends are not significant (for regular pores $p = 0.39$, for irregular pores $p = 0.07$), and (iii) the volume of elongated pores decreases continuously in the S-layer while in the U-layer it decreases sharply (during the first 20 mm of rain) to a smaller value around which it keeps oscillating until the end of the second rain.

The cumulative pore-size distributions of the S- and the U-layers are shown in Figure 4. The macroporosity of both layers shows a strong decrease in the frequency of the largest pores while the frequency of the smallest is almost constant and sometimes even increases. The distributions depend on the processes leading to the decrease of macroporosity. The largest pore-size classes experience only a loss (clogged, broken or compressed pores that decrease their sizes) while the smallest may balance their losses with gains from the coarser classes.

The general trends seem to indicate the occurrence of two different sets of processes in the two layers.

The change in the U-layer is more rapid than that in the S-layer and initially more intense. This seems to contradict any expected behaviour because the S-layer is exposed to the direct impacts of raindrops. The U-layer can be disturbed mainly by the pressure wave which, once generated by drop impact, moves through the soil preferentially destroying the largest pores (this accords with the fact that the total force acting on larger pores is larger than the one acting on smaller pores at any given depth). Other processes, such as slaking of

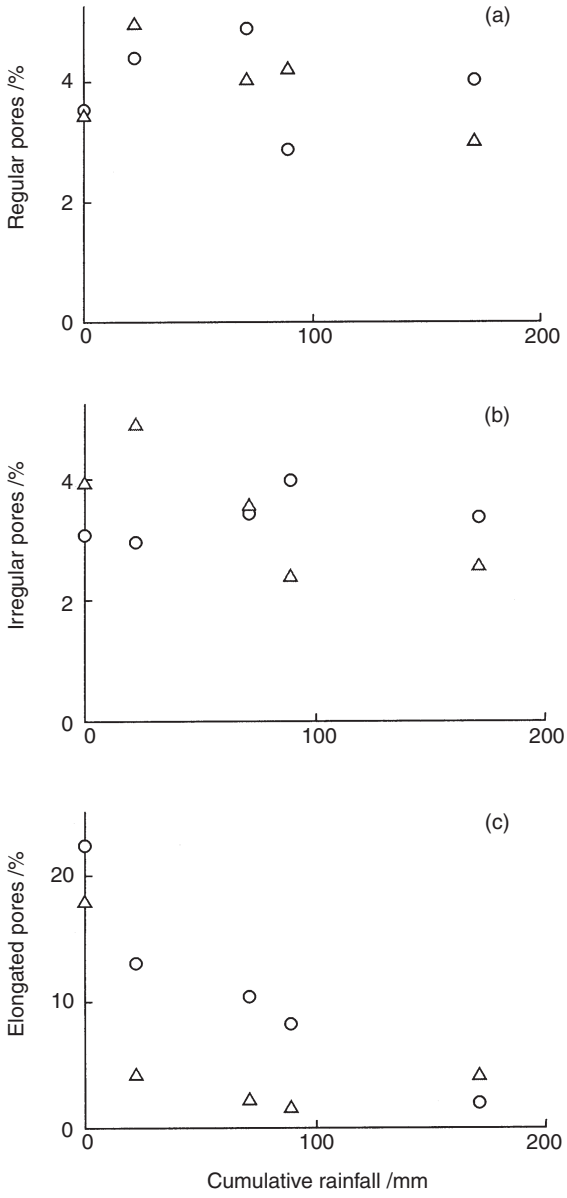

Figure 3 Relationships between area percentages of (a) regular pores, (b) irregular pores and (c) elongated pores obtained by image analysis of thin sections from soil samples of the S-layer (0–3 cm) (○) and the U-layer (3–6 cm) (△) at consecutive time intervals during simulated rain and the cumulative rain rate.

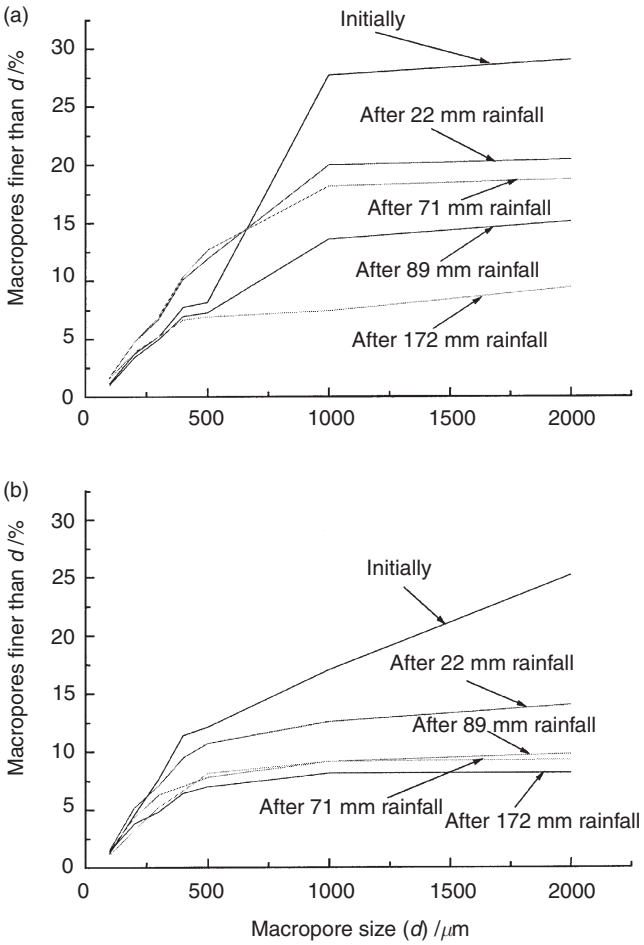

Figure 4 Cumulative pore-size distributions obtained by image analysis of thin sections from samples of (a) the S-layer (0–3 cm) and (b) the U-layer (3–6 cm) at four consecutive time intervals during the simulated rain (respective cumulative rain rates are shown).

aggregates, can also affect U-layer porosity but in this case regardless of pore sizes. In fact, however, the observed porosity reduction was mainly due to destruction of the largest pores (Figure 4b), supporting the pressure wave hypothesis.

To understand clearly the processes and the factors that regulate the presence and dynamics of this pressure wave we must examine the behaviour of the forces generated by drop impacts. Those forces are applied by numerous individual raindrops in a fairly complex manner (Harlow & Shannon, 1967), causing an uneven distribution of pressure. The impact area can be considered as a point where a given pressure is produced. The pressure is a pulse (from zero before the impact, through its peak value, back to zero again in less than a tenth of a second). The pressure wave so generated travels into the soil and expands as the distance between its front and the impact point increases. The intensity of a spherical pressure wave decreases with the square of such a distance. As there are many surface impacts during rain, the spherical pressure waves interfere and produce a plane pressure wave. If the medium in which the wave is expanding does not react then the wave will keep a constant intensity. This is not the case for soil. Its behaviour is partly elastic, when the drop rebounds as droplets often incorporating grains of soil (Styczen & Høgh-Schmidt, 1988), and partly inelastic. The latter is shown by the reduction of pore size, which means that the grains have been rearranged and small volumes of soil compacted, i.e. work has been done by the pressure wave. The wave is also dissipated by sound, friction and heat. Regarding the transmission of the pressure wave, one must remember that the denser is the soil (i.e. the

less the porosity) the more effective is the transmission (smaller reduction of pressure intensity) because there are more particle-to-particle contacts and fewer empty volumes where particles can move.

This leads us to propose the following 'ideal' succession of processes. When it first rains on a soil that has uniform porosity at all depths (at least, within the upper 10 cm), the porosity corresponding to the uppermost soil is reduced whereas below it is scarcely affected because the pressure wave is poorly transmitted in the still very porous uppermost material. As the surface porosity decreases, the pressure wave propagates itself more efficiently so that deeper pores are more and more affected and reduced in size. This progressive transmission of the effect of drop impacts deeper into the soil will obviously end at some depth where the transmitted pressure wave has lost most of its intensity. If larger pores are weaker than smaller pores in the face of disruption by the pressure wave then this process is further amplified.

Let us now return to the S- and U-layer. In the case of our observations the S-layer was less porous (with smaller elongated pores) than the U-layer. If its initial porosity was small enough to allow a good transmission of the pressure wave then the number and size of its larger pores would decrease dramatically.

Predicting the effect of rain on soil macropores

Let us now examine how well the EP model describes the data collected in this experiment, and how the above discussion contributes to a better description of the behaviour of porosity. Trends shown by the S-layer closely resemble the trends shown by Panini *et al.* (1997), even if they do not coincide. The reason for this can be found in the factors influencing the coefficients α, b and P_{ES0} of Equation (4). The coefficient P_{ES0} depends on the initial conditions that characterize the state of the soil surface (i.e. the initial volume of elongated pores in the structurally sealed layer). Hence it can take different values. The coefficient α represents the fraction of the soil surface affected by deposition processes: it may vary rapidly if the soil is initially unaffected by depositional seal. The coefficient b is originally introduced as a proportionality factor that depends on the ratio between 'actual sediment flow, transported by infiltrating water towards the macropores' and the rate of soil detachment. This ratio is not a constant and may vary with sediment load in the runoff and soil detachment depending on the characteristics of the rain as well as on those of the soil. It is defined (Panini *et al.*, 1997) as

$$b = \frac{a(P_{EL} - P_{ES})}{\delta}, \tag{10}$$

where P_{ES} is the elongated porosity (area per cent) in the S-layer sealed 'depositionally', P_{EL} is the elongated porosity in the underlying layer, and δ is the bulk density.

As above, the EP model supposes that the underneath layer of soil was unaffected by raindrop impacts, and P_{EL} was considered constant. This is now questioned by the dynamics in the U-layer (Figure 3c). Let us try to modify the equations accordingly.

The behaviour of the U-layer differs from that of the S-layer because of the following processes: (i) no sample shows a depositional seal thick enough to affect the porosity 3 cm under the soil surface; (ii) drop impact is replaced by the pressure wave (which will be substituted by impact energy – derived by considering pressure intensity proportional to energy by means of a proportionality coefficient that depends on soil depth and on the soil transmissivity, i.e. bulk density, macroporosity, etc.).

Let us refer to Equation (6). Item (i) reduces α to zero, whereas (ii) causes κ_E to be substituted by another parameter, κ'_E, while the energy of drop impact becomes an estimator of the energy (or pressure) wave. In other words, Equation (6) formally reduces to one of its components, i.e. to Equation (2). This leads to the following equation for the variation of elongated porosity in the U-layer (P_{EU}):

$$\Delta P_{EU} = 15.2\{1 - \exp(-11E)\}. \tag{11}$$

This equation has implications for the S-layer. Its governing equation can no longer be Equation (6). In actual fact, the coefficient b in Equations (1), (3) and (6) varies as follows, obtained substituting Equation (11) into Equation (10):

$$b = \frac{a[P_{EL,0} + P_{EL,1}\{1 - \exp(-k'_E E)\} - P_{ES}]}{\delta}, \tag{12}$$

where $P_{EL,0} + P_{EL,1}$ is the initial elongated porosity of the underneath layer and $P_{EL,0}$ is its final one.

If we merge Equations (12) and (6) we can obtain in principle a better description of the behaviour of porosity. Actually the speed at which the largest macropores are reduced in size during rainfall (U-layer variations are fast) will make it scarcely visible and the simplification proposed in the EP model might still hold. The equations are the following ones:

$$\Delta P_E = \{0.008\exp(-0.012E) + 0.0013\}7.36E + 6.3\{1 - \exp(-0.16E)\} \tag{13}$$

and

$$\Delta P_E = \{0.014\exp(-0.006E) + 0.0019\}3.2E + 3.3\{1 - \exp(-0.42E)\}, \tag{14}$$

where Equation (13) is relative to the data collected during these rainfall experiments while Equation (14) describes the observations of Panini *et al.* (1997). The numbers that multiply E are detachabilities (respectively 7.36 and 3.2 g J^{-1}); energy E is in J m^{-2}. The two exponents do not contain detachability because here energy stands as a proxy for the intensity of the pressure wave travelling inside the soil or of the impact pressure. Figure 5 shows trends and data. Notice that the small hump shown by both the interpolating lines at about $E = 100$–300 J m^{-2} is the effect of Equation (12).

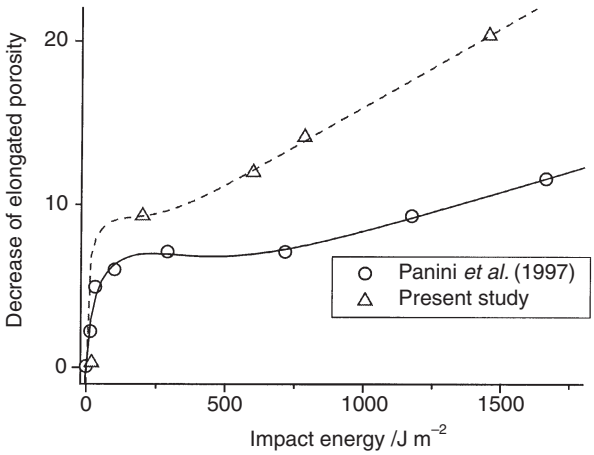

Figure 5 Relationships between the decrease of elongated porosity and the raindrop impact energy in the S-layer when the U-layer has a decreasing porosity: solid line: Equation (14); dashed line: Equation (13).

Before commenting on the values of the parameters of the two new equations, we must state that, given the small number of observations and the large number of parameters to estimate, the results are not unique if some measurement error is admitted. It is indeed possible to obtain an even better match with different values of the parameters. But the range over which the values produce acceptable behaviour is fairly small. For example, the first exponential must be characterized by a small value of the coefficient multiplying E. For instance, in Equation (13) the parameter, the value of which is 0.012, cannot be larger than 0.020 otherwise the relationship does not show any effect of the dynamics of the layer beneath. The two equations show that the corresponding parameters have values close to each other or at least congruent – the differences all lay within a factor of 2, and it is always Equation (13) that has larger parameter values. The fact that the coefficient multiplying E in the first exponential of both equations is so far from the equivalent value shown in Equation (11) might depend on physical reasons. Equation (11) does not distinguish between what happens under depositional and under structural seal, whereas Equations (13) and (14) use the same dynamics but refer to what happens under the depositional seal. The depositional seal tends to develop in local depressions where water accumulates. When water is standing above the soil surface, it substantially adsorbs the energy of impacting drops (Palmer, 1963; Torri *et al.*, 1987). Such a difference might be responsible for the differences between parameter values. Another explanation may lie in the differences in pore-size distribution between the two layers. We stated earlier that the largest pores are generally more affected by the pressure wave than smaller pores. The U-layer was initially characterized by a large volume of large pores compared with the S-layer. Hence, if the largest pores are also the weakest then the first exponential of Equation (13) must be characterized by a smaller value of the coefficient of energy than in Equation (11). This might explain a large part of the differences between the two coefficients of E.

Alternatively, the differences can be explained by measurement or procedural errors or both. For example, if the second value of the U-elongated porosity is flawed (i.e. too small), then Equation (11) could become

$$\Delta P_{EU} = 15.4\{1 - \exp(-0.006E)\}, \qquad (15)$$

with an exponent well in the range of the coefficients of E as shown in Equations (13) and (14).

Pore-size distribution and fractal dimension

The equations discussed above represent the dynamic behaviour of elongated porosity but they give us a quantitative tool for dealing with only one aspect of the pore system. Nothing can be said about the pore-size distribution. Such knowledge can be acquired if we study the dynamics of the fractal dimension of the pore volume because it represents the exponent of the power function fitting the cumulative number–size distribution. The problem, as usual, is the small number of observations (only five time frames). Hence, we first need to identify a possible type of interpolator to reduce the range of choices.

In the previous section we have seen that there is a substantial change during which the U-layer reaches its minimal porosity under the given rainfall conditions, while the S-layer reaches a situation of steady modification – where changes continue to accumulate but at a constant rate (the oblique asymptote represented by the accretion of the depositional seal). Hence we need two different types of interpolators. The changes in the pore system in the U-layer must end quickly, and so the fractal dimension must become a constant after a time. The S-layer keeps modifying, hence the fractal dimension must also continue to modify. Interpolators such as those of Equation (3) for the S-layer and Equation (11) for the U-layer lead to the following results for the pore volume fractal dimension:

$$\text{S-layer: } \Delta D_V = 0.03D + 0.14\{1 - \exp(-13D)\} \qquad (16)$$

and

$$\text{U-layer: } \Delta D_V = 0.42\{1 - \exp(-3.2E)\}. \qquad (17)$$

Figure 6 shows the increase of the pore volume fractal dimension as a function of raindrop impact energy together with the matching of Equations (16) and (17) to the respective data. We can conclude that (i) the processes causing reduction of porosity also cause differences in the spatial distribution of the macropores (more homogeneous pore system with less connected macropores and more mineral soil volume served by each macropore per unit volume), and (ii) this change can be described by equations of the same type as those used for the elongated porosity. As discussed before, regarding the net loss of macropores from the larger size classes, both the

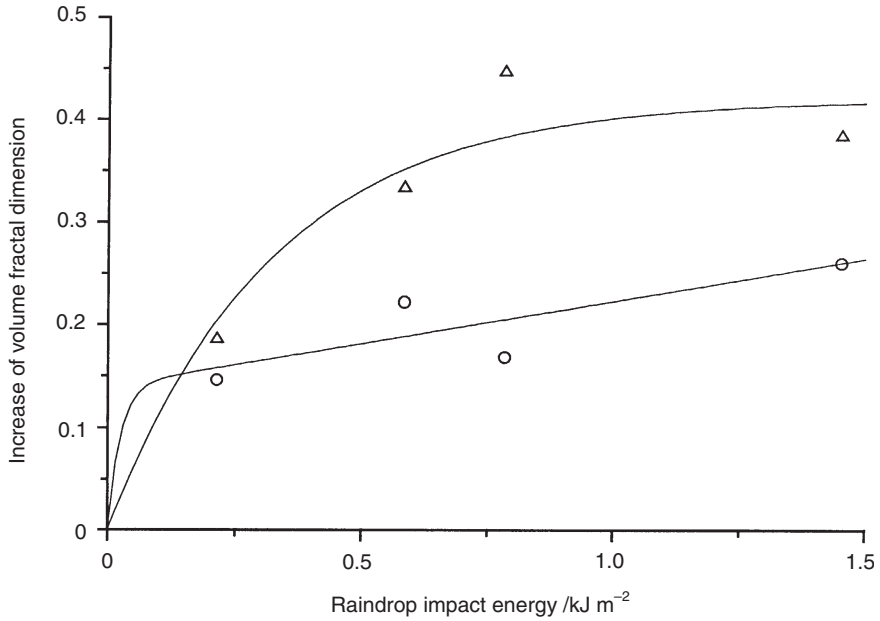

Figure 6 Relationships between the increase of pore volume fractal dimension and the raindrop impact energy in the S-layer (○) and in the U-layer (△).

Table 1 Fractal dimensions of the pore surface roughness (D_S) and the pore volume (D_V) at consecutive time intervals during the simulated rainfall

		D_S								D_V	
		Macroporosity		Regular pores		Irregular pores		Elongated pores		Macroporosity	
Cumulative rain /mm	Soil layer depth /cm	Mean	SD	Mean	SD	Mean	SD	Mean	SD	Mean	SD
0	0–3	2.534	0.012	2.539	0.010	2.197	0.014	2.181	0.052	2.576	0.305
	3–6	2.541	0.008	2.550	0.010	2.137	0.015	2.207	0.072	2.490	0.097
22	0–3	2.562	0.011	2.570	0.004	2.157	0.008	2.160	0.005	2.722	0.048
	3–6	2.538	0.013	2.542	0.002	2.141	0.019	2.227	0.078	2.675	0.205
71	0–3	2.547	0.017	2.555	0.006	2.123[a]	0.017	2.191	0.044	2.798	0.174
	3–6	2.553	0.019	2.557	0.015	2.129	0.036	2.077	0.031	2.823	0.214
89	0–3	2.536	0.002	2.574	0.002	2.105[a]	0.011	2.130	0.028	2.744	0.144
	3–6	2.558	0.006	2.555	0.015	2.112	0.020	2.028	0.110	2.936	0.015
172	0–3	2.565	0.023	2.568	0.016	2.139	0.027	2.080	0.008	2.836	0.444
172	3–6	2.547	0.007	2.553	0.013	2.099	0.004	2.220	0.045	2.873	0.183
Structural seal	0–3	2.558	0.005	2.550	0.009	2.186	0.030	2.179	0.041	2.820	0.199
	0–1.5	2.601[a]	0.013	2.586[a]	0.010	2.165	0.009	2.246	0.133	2.808	0.055
172											
Depositional seal	0–3	2.569[a]	0.006	2.568	0.010	2.148	0.024	2.216	0.054	2.730	0.150
	0–1.5	2.578[a]	0.016	2.555	0.018	2.297	0.073	2.174	0.094	2.875	0.1245

[a]Marked values are significantly different from the initial ones at $P < 0.05$.

decrease of elongated porosity and the increase of the pore volume fractal dimension are two aspects of the same process of loss of porosity. The increase of D_V means a decrease of heterogeneity that can be associated with loss of macropores from the larger size classes as a consequence of compaction.

Table 1 shows the values of the fractal dimension of the pore surface roughness (D_S) and the fractal dimension of the pore volume (D_V). Similar fractal dimensions, ranging roughly between 2.1 and 2.2, i.e. close to 2.0 which is the fractal dimension of a smooth surface, represent the surfaces of irregular and elongated pores. While values for irregular and elongated pores decrease slightly with accumulated rain, the surfaces of regular pores, which are rougher and with fractal dimensions ranging between 2.5 and 2.6, seem to become still rougher.

The fractal dimension of the pore volume increases significantly during the rain, i.e. the pore system becomes more homogeneous, since more heterogeneous pore systems tend

to have smaller values of D_V (Anderson *et al*., 1996). The relative increase (i.e. difference from the respective initial value) is continuous in the U-layer, whereas in the S-layer it is sharp (during the first 22 mm of rain). Examination of the fractal dimensions of structural and depositional seals (0–1.5 cm) shows that the structural seals are characterized by rougher pore surfaces and more heterogeneous pore systems than those in the depositional seals.

Conclusions

Rain affects soil macroporosity to a depth of at least 6 cm, but the way and the rate at which macroporosity decreases at the surface (0–3 cm) differ from those in the layer beneath (3–6 cm). Hence, different mechanisms are to be considered when modelling the processes in these two layers. In both layers most of the variation in macropores is due to loss of elongated porosity. The fractal dimension of the pore volume increases in both layers. These observations were used for improving the set of equations first given by Panini *et al*. (1997).

The reduction of porosity in the U-layer seems to be due to the pressure wave generated by the impacts of raindrops at the soil surface. By supposing the pressure intensity at a given depth to be proportional to the kinetic energy of the impacting drop we found an equation describing the reduction of elongated porosity. This has led us to modify one of the assumptions originally made by Panini *et al*. (1997): the proportion of elongated pores below the depositional seal is not constant but varies because of the pressure wave. Hence, the parameters b of the equations of Panini *et al*. (1997) can no longer be considered constant. Once the equations are modified accordingly, the observed data, including those found by Panini *et al*. (1997), are better interpolated.

The fractal dimensions of the pore volume increase regularly, with an oblique asymptote in the surface layer and a horizontal asymptote in the deeper layer. The way in which soil macropores are distributed in the soil volume changes during the rain, the pore system becoming more homogeneous with smaller and less connected macropores.

The application of physico-mathematical techniques to the dynamics of macropores represents a powerful tool for understanding the processes and their interlinkages. Unfortunately, many data are required, while the processes show growing complexities, leading to uncertain evaluations of the parameter values.

Acknowledgements

We thank M. Del Sette, M.S. Yañez, L. Borselli and S. Giampaolo for their invaluable help in planning and conducting the experiments, and Dr O. Grasselli, in charge of the Fagna Agricultural Experimental Centre, for her support in setting up the experiment. S. Rousseva gratefully acknowledges the ICTP Programme for Training and Research in Italian Laboratories for a fellowship to work at Istituto Sperimentale per lo Studio e la Difesa del Suolo, Firenze. We are grateful to the Editors for their improvement to the script. Part of this work was funded by the project EU-ENV4-CT97-687 (MWISED).

References

Anderson, A.N., McBratney, A.B. & FitzPatrick, E.A. 1996. Soil mass, surface, and spectral fractal dimensions estimated from thin section photographs. *Soil Science Society of America Journal*, **60,** 962–969.

Bielders, C.L. & Baveye, P. 1995. Processes of structural crust formation on coarse-textured soils. *European Journal of Soil Science*, **46,** 221–232.

Boiffin, J. 1984. *La degradation structurale des couches superficielles du sol sous l'action des pluies*. Thèse de Docteur-ingénieur, Institut National Agronomique, Paris-Grignon.

Borselli, L., Torri, D. & Poesen, J. 2001. Impact of rainwater quality on infiltration, runoff and interrill erosion processes. *Earth Surface Processes and Landforms*, **26,** 329–334.

Bouma, J., Jungerius, A., Boersma, O.H., Jager, A. & Schoonderbeek, D. 1977. The function of different types of macropores during saturated flow through four swelling soil horizons. *Soil Science Society of America Journal*, **41,** 945–950.

Brandt, C.J. 1989. The size distribution of throughfall drops under vegetation canopies. *Catena*, **16,** 507–524.

Bresson, L.M. & Boiffin, J. 1990. Morphological characterisation of soil crust development stages on an experimental field. *Geoderma*, **47,** 301–325.

Droogers, P., Stein, A., Bouma, J. & de Boer, G. 1998. Parameters for describing soil macroporosity derived from staining patterns. *Geoderma*, **83,** 293–308.

Ellison, W.D. 1947. Soil erosion studies. Part II: Erosion hazard by raindrop splash. *Agricultural Engineering*, **28,** 197–201.

FAO–UNESCO 1990. *Soil Map of the World, Revised Legend*. FAO, Rome.

Farres, P. 1978. The role of time and aggregate size in the crusting process. *Earth Surface Processes*, **3,** 243–254.

Harlow, F.H. & Shannon, J.P. 1967. The splash of a liquid drop. *Journal of Applied Physics*, **38,** 3855–3866.

Laws, J.O. 1941. Measurements of the fall velocity of waterdrops and raindrops. *Transactions of the American Geophysical Union*, **22,** 709–721.

Mandelbrot, B.B. 1982. *The Fractal Geometry of Nature*. W.H. Freeman, San Francisco, CA.

Miedema, R., Pape, T. & van de Waal, G.J. 1974. A method to impregnate wet soil samples, producing high quality thin sections. *Netherlands Journal of Agricultural Science*, **22,** 37–39.

Mualem, Y., Assouline, S. & Rohdenburg, H. 1990. Rainfall induced soil seal. C. A dynamic model with kinetic energy instead of cumulative rainfall as independent variable. *Catena*, **17,** 289–303.

Murphy, C.P. 1986. *Thin Section Preparation of Soils and Sediments*. A B Academic Publishers, Berkhamsted.

Onstad, C.A. 1984. Depressional storage on tilled soil surfaces. *Transactions of the American Society of Agricultural Engineers*, **27,** 729–732.

Pagliai, M., Bisdom, E.B.A. & Ledin, S. 1983. Changes in surface structure (crusting) after application of sewage sludge and pig slurry

to cultivated agricultural soils in Northern Italy. *Geoderma*, **30,** 34–53.

Pagliai, M., La Marca, M., Lucamente, G. & Genovese, L. 1984. Effects of zero and conventional tillage on the length and irregularity of elongated pores in a clay loam soil under viticulture. *Soil and Tillage Research*, **4,** 433–444.

Palmer, R. 1963. The influence of a thin water layer on water drop impact forces. *International Association of Hydrological Sciences*, **65,** 141–148.

Panini, T., Salvador Sanchis, M.P. & Torri, D. 1993. A portable rain simulator for rough and smooth morphologies. *Quaderni di Scienza del Suolo*, **5,** 47–58.

Panini, T., Torri, D., Pellegrini, S., Pagliai, M. & Salvador Sanchis, M.P. 1997. A theoretical approach to soil porosity and sealing development using simulated rainstorms. *Catena*, **31,** 199–218.

Poesen, J. & Savat, J. 1981. Detachment and transportation of loose sediments by raindrop splash. Part II: Detachability and transportability measurements. *Catena*, **8,** 19–41.

Roth, C.H. 1997. Bulk density of surface crust: depth functions and relationships to texture. *Catena*, **29,** 223–237.

Styczen, M. & Høgh-Schmidt, K. 1988. A new description of splash erosion in relation to raindrop sizes and vegetation. In: *Agriculture: Erosion Assessment and Modelling* (eds R.P.C. Morgan & R.J. Rickson), pp. 147–184. Commission of the European Communities, Brussels.

Tackett, J.L. & Pearson, R.W. 1965. Some characteristics of soil crusts formed by simulated rain. *Soil Science*, **99,** 407–413.

Torri, D., Sfalanga, M. & Del Sette, M. 1987. Splash detachment: runoff depth and soil cohesion. *Catena*, **14,** 149–155.

Torri, D., Ciampalini, R. & Accolti Gil, P. 1998. The role of soil aggregates in soil erosion processes. In: *Modeling Soil Erosion by Water* (eds J. Boardman & D. Favis-Mortlock), pp. 231–242. Springer-Verlag, Berlin.

West, L.T., Chiang, S.C. & Norton, L.D. 1992. The morphology of surface crusts. In: *Soil Crusting – Chemical and Physical Processes* (eds M.E. Sumner & B.A. Stewart), pp. 73–92. Lewis Publishers, Boca Raton, FL.